Received: 1 June 2017 | Revised: 23 November 2017 | Accepted: 23 November 2017

DOI: 10.1002/stc.2134

RESEARCH ARTICLE

WILEY

Local effects induced by dynamic load self-heating in NiTi wires of shape memory alloys

S. Casciati[1] | V. Torra[2] | M. Vece[3]

[1] DICAr, School of Architecture, University of Catania at Siracusa, P.za Federico di Svevia, Siracusa 96100, Italy

[2] Polytechnic University of Catalonia, Villarroel 162, E-08036 Barcelona, Spain

[3] R2M Solution S.r.l., Via Fratelli Cuzio 42, 27100 Pavia, Italy

Correspondence
M. Vece, R2M Solution S.r.l., Via Fratelli Cuzio 42, 27100 Pavia, Italy.
Email: miche.vece@gmail.com

Summary

The use of shape memory alloys wires in dampers devices for Civil Engineering applications is well documented in the literature. This paper develops a critical discussion on the wire macroscopic behavior and on the associated temperature effects with emphasis on the wire diameter. Vibration damping requires the absorption of mechanical energy and its conversion to heat via the action of hysteresis cycles. The experimental study is carried out on NiTi wires of different diameters. The flat cycles shown by thin wires (i.e., 0.5 mm of diameter or less) and the nonclassical S-shaped cycles (e.g., for diameter 2.46 mm) establish clear differences in the response of the samples. For this reason, a supplementary investigation is here reported to show that the flat cycles are coherent with the classical treatment of shape memory alloys as a first-order phase transition, but the S-shaped cycles of thick wires can be associated to an anomaly in the heat capacity.

KEYWORDS

damping, hysteresis, self-heating, shape memory alloys, temperature effects

1 | INTRODUCTION

Many physical systems show "phase transitions," which are characterized by anomalies in one of the thermodynamic potentials (such as the free energy) and, hence, by discontinuities in their derivatives. The pioneer work by P. Ehrenfest[1] classified phase transitions according to whether the first, second, and so on derivative of the free energy shows a discontinuity. They were named first, second, and so on "order transitions," respectively. Because the first derivative of the relevant thermodynamic potential is discontinuous, in the case of a first-order phase transition, such a phase transition will usually come with a latent heat. Nowadays, it is well known that not only discontinuities but also anomalies at the phase transition point have to be considered. All higher order phase transitions are grouped as critical or "continuous phase transitions." This term was introduced by Landau in his classic paper on the theory of phase transitions.[2]

Shape memory alloys (SMAs) are smart materials with a wide range of practical and potential applications. Some of the proposed exploitations were devoted to health solutions (e.g., in orthodontic applications). SMA elements were also studied for dampers in civil engineering, as well as potential components in morphing. The particular properties of SMA are related to a martensitic phase transition (MT). This is recognized to be a first-order transition with hysteresis between the metastable solid phases.

The experimental analysis of SMA wires shows a hysteretic behavior both in stress–strain or strain–temperature representations. Indeed, a series of repeated loading–unloading cycles in stress–strain coordinates shows a monotonic SMA creep and a practical reduction of the available deformation. In the temperature-induced transformations, without

external stresses, the interaction between martensite variants expands the transformation temperatures interval to more than 30 K. These interactions largely increase the difference between martensite start temperature (M_s) and martensite finish temperature (M_f). For each maximal stress and temperature, the creep increases in an exponential shape to saturation. This and the larger difference between M_s and M_f suggest some nonclassical behavior of SMAs in comparison with conventional phase transitions with an extremely reduced temperature span. As a classical result, the alloy composition and the undergone heat treatments characterize the transformation and their behavior.[3]

Interest in SMAs has been increasing over the last three decades due to their potential applications.[4,5] This interest has recently been enhanced by the inclusion of university courses on smart materials in the engineering field, but, thus far, SMAs have mainly been applied to the health field. For instance, the classical NiTi alloys[6,7] have been attracting interest due to their biological compatibility in practical situations (i.e., NiTi functions as an innocuous substance in the human body). In recent years, Ti-based alloys (avoiding Ni) has been in continuous research by the Miyazaki group in Tsukuba.[8–11] Several SMA applications are on the market such as stents, surgical tools, orthodontic wires or bolts, and elements for bone/teeth reconstruction. The number of useful and efficient applications has increased in other fields such as in automotive and consumer electronics,[12–14] but it still includes a relatively small number of successful applications.

The study of NiTi SMA samples covers their properties related to the memory effect, due to a martensitic transformation between the solid phases. Such a study shows some effects that can affect their exploitations. In the literature,[15–20] the alloy capability to carry out significant deformations associated to the phase transformation is well investigated. Even if single crystals produce more significant strains than in the classical polycrystalline wires, the interaction between the join-grains results in regarding an 8% deformation as high.

Several investigations were devoted to the pseudoelastic behavior of NiTi SMA wires and bars. The practical interest of several applications, however, relies on working cycles induced by stress (i.e., stress-induced transformation) or temperature (i.e., temperature-induced transformation). In addition, the "fatigue" effect of the samples on cycling has to be emphasized.[21–23] After repeated loading–unloading cycles, the material suffers a permanent increase of length, known as the SMA creep, due to the residual deformation of the sample and the retained martensite induced by the working stress (i.e., close to 600 MPa).

In this work, the evolution of the mechano-cyclic creep is investigated for different, conventional diameters of the wire. Attention is paid to the initial training, which consists of 100 sinusoidal loading–unloading cycles to homogenize the properties of the wire samples and the subsequent behavior. The training leads the samples to show similar and "reproducible" characteristics during the tests. The experimental campaign shows that thinner wires (i.e., 0.2- or 0.5-mm diameter) at slow rate work in flat cycles as expected for a first-order transformation at constant stress (i.e., a classical first-order transition), whereas thick wires (i.e., 2.46-mm diameter) convert the initial horizontal cycles in S-shaped loops.

Furthermore, the thermodynamic study of S-shaped cycles suggests a dependence of the heat capacity on strain when compared with the expected actions of latent heat in flat cycles. Results of tests on thinner and thick wires are reported to analyze the thermal behavior for different working cycles.

In summary, this paper reports a study of the SMA mechano-cyclic creep and the realization of flat or S-shaped stress (strain) curves. In this regard, the reader is also addressed to previous studies.[24–26] In particular, Zhu and Zhang[24] presented a sophisticated thermodynamic model and test results that successfully explain many phenomena reported in this paper, including self-heating and self-cooling in the loading process, the different slopes of thin and thick wires, and the temperature effect.

2 | EXPERIMENTAL SETUP AND THEORETICAL BACKGROUND

2.1 | Laboratory facilities

The material specimens for the tests reported in this paper were acquired from standard furnishers. The use of SMA in dampers for bridge stayed cables requires wire portions of several meters of length situated between the stayed cable and the platform or, eventually, connecting the cables. In addition, the dampers preparation requires the purchase of several hundreds of meters with reliable properties. Some sophisticated heat treatments, suitable for materials science laboratories using short samples, remain completely out of the end user capability in this kind of applications.

The authors used a NiTi alloy in the pseudoelastic state, supplied in several orders and years (from 2007 to 2015) by Memry (CT, USA), a division of SAES Getters, and previously by Special Metals Corp (2004–2007). Wires of two diameters are mainly studied, which are provided in the straight super elastic state.

In the "A" wires, the surface of the samples is finished in a light-gray oxide surface with a diameter of 2.46 mm (Figure 1), and for the type labeled "B," with a diameter of 0.5 mm, the surface is in black oxide. According the supplier's certificates, the austenite start temperatures (A_s) are similar, that is, 247 and 243 K, respectively. The certification by the supplier indicated that the nominal wire composition was about 55.93 wt.% of Ni balance Ti. The composition also includes other minor components such as 270 ppm of C, 234 ppm of O, and reduced quantities (<0.01 wt.%) of several elements (i.e., Si, Cr, Co, Mo, W, Nb, Al, Ba, H, and Fe). Moreover, other thinner diameters of 0.2 and 0.1 mm with black oxide surfaces, also furnished by SAES Getters, were tested. The main features of the tested NiTi samples are summarized in Table 1.

The study was conducted using the Mini Bionix II (Figure 1a), situated in a protected laboratory with its own air conditioning system that maintains the working temperatures near 293 K. To investigate local temperature effects on the samples, two sets of K-thermocouple wires from OMEGA with a diameter of 0.005 mm were used wrapped to the samples, as shown in Figure 1b. Their sampling rate is up to 6.5 p.p.s, and their positions are provided in Table 1. It is worth noting that the thermocouple wires in each position covered 1 cm of the specimen length. Such a wrapping prevents from localized compositional changes induced by spot welding. The length of the K-thermocouple covers around 2–4 mm. The contact cannot be considered as a point, and this introduces more uncertainty in the readings, that is, noise. An OMEGA zero point (Figure 1b) was used as a reference temperature: The signal was digitized at a controlled time up to 2 p.p.s. by a proprietary program using a DMM Agilent U1251A and stored in a PC for further analysis.

Special grips were mounted in carrying out the planned tests. They allow the introduction of a traction that avoids the parasitic compressive effects created by the progressive SMA creep. In particular, the increased length, which induces compression in classical grips, was avoided by U element in the bottom part of the grip, which permits slip, and compensates a creep up to 20 mm.

The stress–strain relation with the associated temperature was central in this work. Figure 2 summarizes the tests carried out in the timeframe of a week. Actually, Figure 2 shows the room temperature against time for several days of work. Each strain peak denotes that a test is carried out following the labeled sequence. In this way, the correlation between the room temperature and the single test response is outlined. Around the equipment, simple protective structures by plastic and cellulose sheets were installed to allow one the investigation of minor transformation steps and smooth-parasitic temperature behaviors by the direct actions of the air-conditioning equipment.

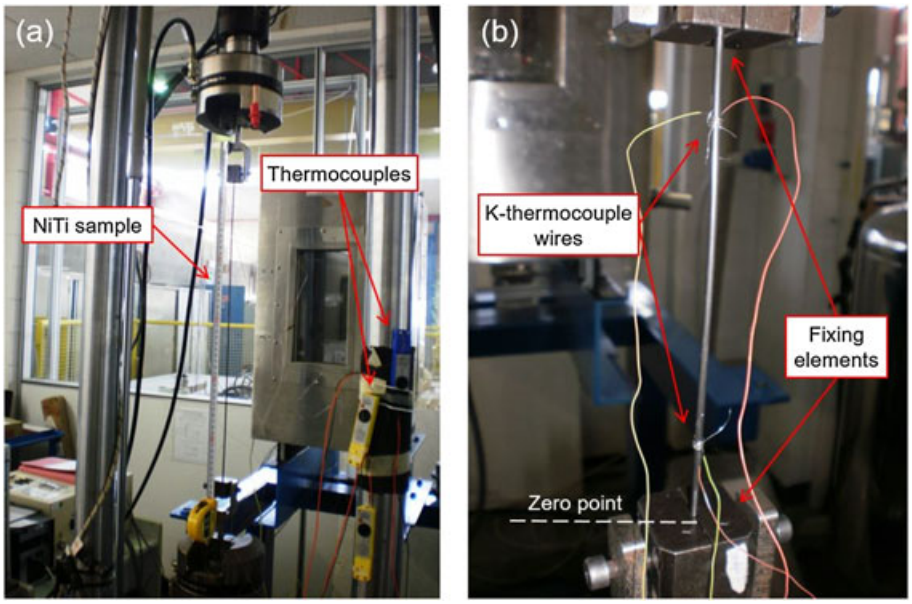

FIGURE 1 Mini Bionix II (a) and focus on zero point in the K-thermocouple system (b)

TABLE 1 Features of the tested NiTi wires

Id sample	Diameter (mm)	Effective length (mm)	Cycling frequency (Hz)	Position of K-thermocouples from the bottom grip (mm)	
				Bottom	Top
A1	2.46	502	0.005	50	480
A2		140		26	122
B1–B2–B3 B4–B5–B6	0.50	175	0.05	38	140
C1–C2–C3 C4–C5–C6	0.20	163	0.1	40	120
D1–D2	0.10	163	0.1	27	136

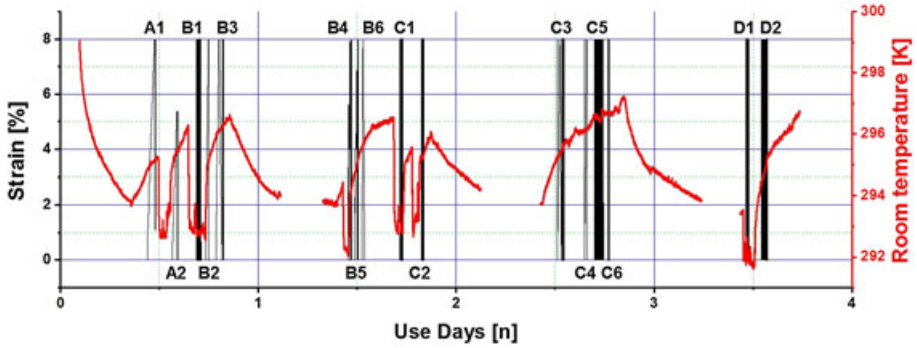

FIGURE 2 Room temperature (top) and strain (bottom) records for loading–unloading cycles on wires of different diameter. The estimated mean temperature was 294 K (21 °C)

2.2 | Governing relations

A thermodynamic approach is easily implemented assuming the specimen as a system, with only one thermodynamic coordinate, of cross-section A. Under progressive external stress, the material experiences a first-order phase transformation, equivalent to an MT. The material converts progressively from parent (austenite) to martensite under an external force ($f_{ext(p \rightarrow m)}$). The specimen length increases from x_p to x_m with an increase of Δx ($\Delta x = x_m - x_p$). The associate strain is $\varepsilon = \Delta x/x_p$, which in a crystallographic transformation, is lower than 10%.

Neglecting the eventual change of the diameter and the associated external pressure effects, the work is easily written by Equation 1 and the specimen dissipates a latent heat. In the retransformation, the external force exhibits a lower value due to the hysteresis, and the length goes back from x_m to x_p with one heat absorption.

When the material specimen converts to martensite, dissipating the latent heat, the entropy moves from S_p to S_m. The realized work in f-x is equal to the heat dissipated in the T-S representation, with T denoting the temperature. By introducing differentials of force and temperature, the work W equals heat Q, and the balance reads as follows:

$$W = df_{coex}\left(x_m - x_p\right) = Q = dT_{coex}\left(S_p - S_m\right). \tag{1}$$

Equation 1 can be rewritten in the form of the Clausius–Clapeyron equation:

$$\left(\frac{df_{coex}}{dT_{coex}}\right) = \frac{S_p - S_m}{x_m - x_p} \tag{2}$$

that is easily converted in its form involving the stresses by dividing by the cross-section area A. The equipment presented in the previous subsection was also appropriate to determine this ratio, known as the Clausius–Clapeyron (C-C) coefficient,[27] which is 6.3 MPa/K for both the "A" and "B" wires.

The C-C equation relates a first-order phase transition with a flat process in the transition at constant force and temperature, as actually experienced for thin diameters wires.

When the hysteresis cycles come with a continuous increase of the force (the S-shaped cycles) associated with the transformation, as for thick diameter wires, the equations have to be reformulated. For the work in a wire, the thermodynamic equations state:

$$TdS = dU - fdx = \left(\frac{\partial U}{\partial T}\right)_x dT + \left(\frac{\partial U}{\partial x}\right)_T dx - fdx = C_x dT + \left(\left(\frac{\partial U}{\partial x}\right)_T\right) dx - fdx, \tag{3}$$

where U is the internal energy and C_x denotes the heat capacity at constant volume.

Having in mind that

$$T = \left(\frac{\partial U}{\partial S}\right)_x; \quad f = \left(\frac{\partial U}{\partial x}\right)_S \quad and \quad U(T,x) = U(S(T,x),x), \tag{4}$$

the second addendum in Equation 3 is written:

$$\left(\frac{\partial U}{\partial x}\right)_T = \left(\frac{\partial U}{\partial S}\right)_x \left(\frac{\partial S}{\partial x}\right)_T + \left(\frac{\partial U}{\partial x}\right)_S = T\left(\frac{\partial S}{\partial x}\right)_T + f = -T\left(\frac{\partial f}{\partial T}\right)_x + f, \tag{5}$$

where the last equality can be obtained only if the transformation is an equilibrium and reversible process (from considering the free energy F).

The resulting expression for Equation 3 is

$$TdS = C_x dT - \left(T\left(\frac{\partial f}{\partial T}\right)_x\right) dx. \tag{6}$$

In a phase coexistence with one S-shaped transformation without a flat process, that is, with a heat capacity C_{coex}, Equation 3 becomes

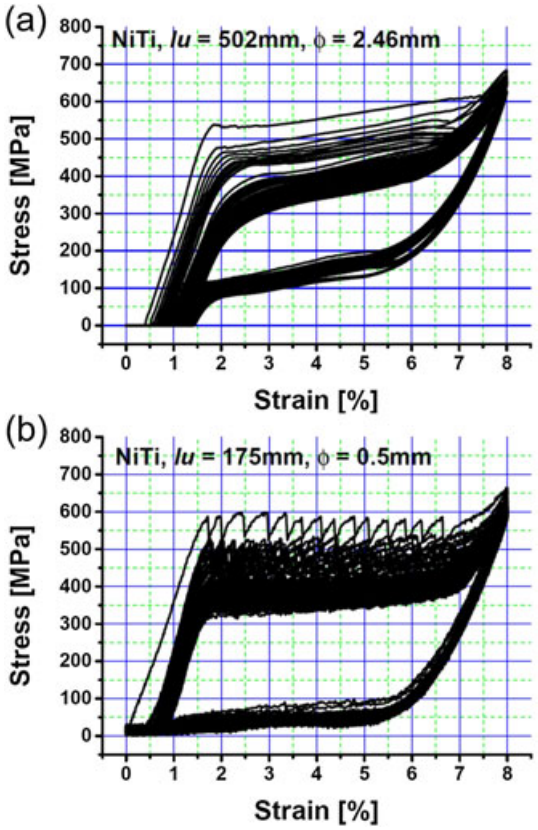

FIGURE 3 Hysteretic behavior for 100 sinusoidal cycles (no preliminary training), for the thick wire (a) and the thin wire (b)

$$C_{coex}dT_{coex} = C_x dT_{coex} - \left(T\left(\frac{\partial f}{\partial T}\right)_x\right)dx_{coex}. \tag{7}$$

Thus, without a flat process, the thermodynamic identity establishes a link between the heat capacity (C_{coex}) and the strain–stress ratio ($(d\varepsilon/d\sigma)_{coex}$) of the specimen, which can be expressed by the following equation[28]:

$$C_{coex} = C_x - \left(T\left(\frac{\partial f}{\partial T}\right)_x\right)\frac{dx_{coex}}{dT_{coex}} = C_x - \left(T\left(\frac{\partial f}{\partial T}\right)_x\right)\frac{dx_{coex}\,df_{coex}}{df_{coex}dT_{coex}}, \tag{8}$$

where T is the internal temperature of the specimen. The term $((df_{coex}/dT)_{coex})$ is the C-C coefficient in Equation 2.

Because $\sigma = f/A$ and $\varepsilon = x_{coex}/x_p$, Equation 5 becomes

$$C_{coex} = B\frac{dx_{coex}}{df_{coex}} = B'\left(\frac{d\varepsilon}{d\sigma}\right)_{coex}. \tag{9}$$

Different series of measurements can be carried out to visualize the heat capacity change with strain. In Sections 4 and 5, a sequence of steps of strain and associated pauses to homogenize the temperatures is adopted. The steps show a particular evolution of the temperature peaks, similar to the evolution of $(dx/df)_{coex}$.

3 | LOADING–UNLOADING CYCLES ON WIRES OF DIFFERENT DIAMETER

Recent studies[28,29] focused on damper applications in civil engineering and outlined some discrepancies in the SMAs hysteretic behavior for wires of different diameters, that is, thick (2.46 mm) and thinner (0.5 mm) wires. Figure 3 shows the particular trend of the hysteretic cycles for the two diameters. Figure 4 gives the associated temperature effects, for two positions close to both ends of the specimens, in the form of time histories. The tests are carried out with 100 sinusoidal cycles, and the ratios between the cycling frequencies agree with the ratio of the wires radius, according to the requirement of having similar losses by heat transfer in cylinders.[28]

Cycle after cycle, the specimen B1, of 0.5-mm diameter and 175-mm length, undergoes a flat transformation (Figure 3b) by the classical first-order transformation realized at constant stress. Of course, in the initial cycles, the

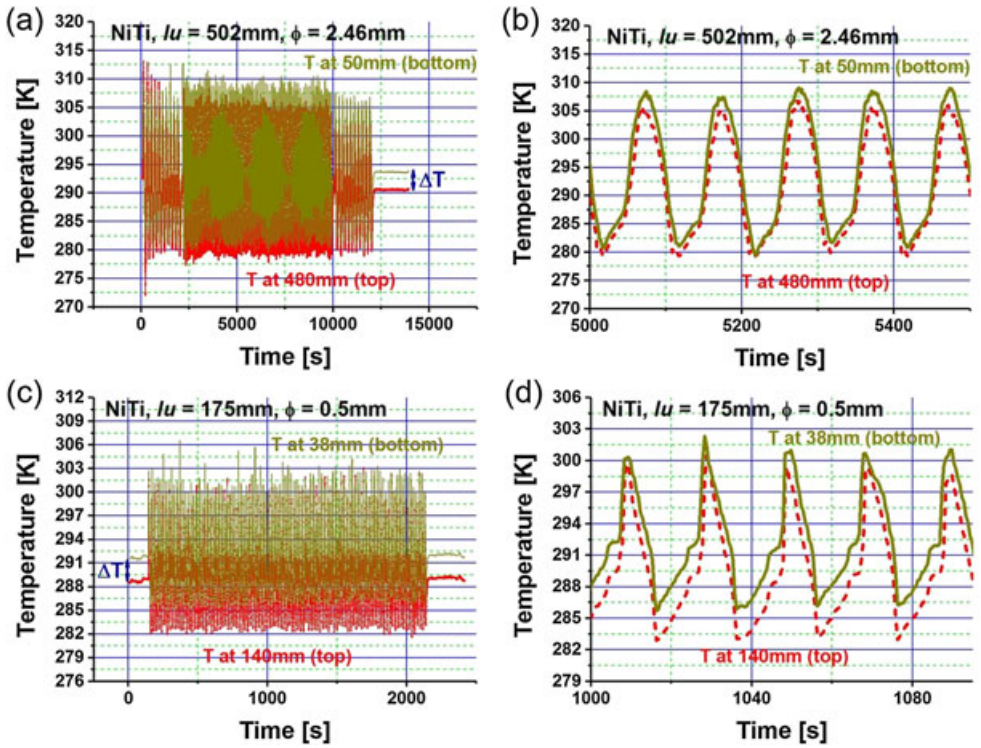

FIGURE 4 Time histories and relative focus for the associated temperature effects: thick wire (a, b) and thin wire (c, d)

transformation showed several jumps associated with the martensite nucleation. On the other side, the specimen A1, of 2.46-mm diameter and 502-mm length, does not work at constant stress but requires a progressive stress increase or decrease. The hysteresis loop assumes an S-shaped aspect (Figure 3a).

The wrapped K-thermocouples produce the temperature signals associated with the specimen loading–unloading training (Figure 4). The measurements outline some transient effects in the temperature. The temperature oscillation was similar for the two different positions in the NiTi wires: top (solid line) and bottom (dashed line). The upper and lower positions of the "A" sample were at 480 and 50 mm from the bottom grip, respectively, and they were at 140 and 38 mm, respectively, for the thinner wire, that is, the "B" sample.

For the "A" sample, which was tested by sinusoidal strain cycles up to a maximum deformation of 8%, the S-shaped cycle (Figure 3a) starts practically at zero and ends near 600 MPa. It is worth noticing that, when the retransformation of the cycle ends at zero stress, a residual martensite appears in the cycles. Pseudoelastic cycles need nonzero stress at the end of retransformation.

This is in contrast with the classical behavior of thinner wires (Figure 3b). The temperature measurements suggest that the transformation process changed from a local dissipation with a "front transformation" to a "distributed transformation," which requires progressively increasing/decreasing load.

The technical relevance in the discrepancy outlined in the shape of the hysteresis cycles becomes evident when one computes the shift of the loop associated with the C-C coefficient (near 6.3 MPa/K in Isalgue et al.[27]). At 273 K (0 °C, winter reference), the C-C induces a reduction of the stresses level for the first-order transition of nearly 125 MPa. Consequently, the wire of diameter 0.5 mm cannot retransform; it only describes the "elastic" part of martensite in the range from 8% to 6% of strain (see Figure 3b). At the same winter reference temperature, the wire of diameter 2.46 mm retransforms from 8% to 3% and can describe partial cycles with hysteresis.

In summary, the thinner wire cannot retransform and remain in martensite, that is, it is unsuitable in cold winter, and the thick wire remains liable for temperatures as low as 253 K (−20 °C) or lower.

Devices mounting SMA components, to be located where sensitive to cold winter effects (i.e., Canada or northern Europa), need elongated S-shaped loops as achievable by higher maximal stress. Strain aging producing maximal stress as 900–1,000 MPa seems a clear technological answer but need a deep study of the fatigue-fracture in strain aged wires.

4 | THICK DIAMETER WIRES: STRAIN STEPS EFFECT

Within the term "temperature actions," one should distinguish two components: the changes of the external temperatures and the self-heating generated by the phase transition with two "simultaneous" effects. The temperature oscillation associated to the transformation and the retransformation and that due to the hysteresis dissipation. In slow cycles, the temperature oscillates from positive to negative. In fast cycles, the effects reduce to a heating that increases with the increasing of the frequency.

The only way to isolate the self-heating features is to increase/decrease the strain of a limited amount and to stop the process to stabilize the consequent transition. The step occurs in 4 s, and 196 s of pause follow. Each step has the duration of 200 s. In this way, one can produce a full cycle. The test is carried out on the virgin specimen (Cycle 1) and on the specimen after the training of 100 sinusoidal cycles (Cycle 101). The recorded data are plotted in Figures 5

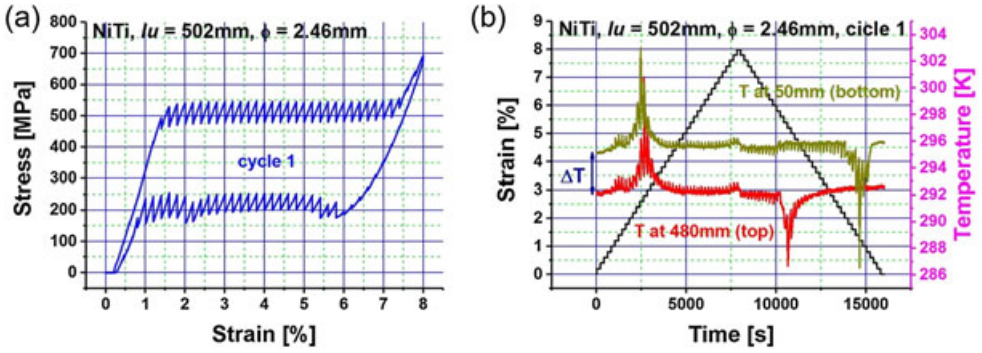

FIGURE 5 Strain steps effect before training: stress against strain (a), and temperatures against time (b)

and 6, respectively. The plots in Figures 5b and 6b offer the time histories of the strain (solid line) and of the temperatures at the bottom (dotted line) and top (dashed line) thermocouples.

When the loading–unloading is carried out before the training, one detects higher peaks temperatures at the time the local transformations appeared in the position of each K-thermocouple. It is worth noticing the bottom delay in the decreasing deformation stage (Figure 5b).

When the loading–unloading is carried out after the training, the temperature peaks are smoothed and the temperature oscillations are no longer localized in time (Figure 6b).

It is worth mentioning that both Cycles 1 and 101 show a flat transformation due to the pauses between steps in the loading/unloading. Of course, the training induced an increase of the creep. Indeed, in Cycle 101 (Figure 6a), the creep was about 1.4% with a significant reduction in the force steps and of the hysteresis width. Moreover, Figure 6b shows a "homogenization" of the associate temperature steps in all parts of the sample. The transformation passes from a local transformation (i.e., a progressive displacement of the parent to martensite interface induced by the strain), recorded separately in the two thermocouples (Figure 5b), to a distributed transformation, that is, a simultaneous transformation in the "complete" sample. Indeed, from Figure 6b, one can see that temperatures registered by both the top and bottom thermocouples are not uniform (there are peaks). Actually, the initial cycles of the transformation were realized via the displacement at the interfaces parent-martensite in the wire. When the interface passes under the K-thermocouple, it appears a "local" maximum of temperature. Later, the transformation seems homogeneous for the whole sample. Thermal signal appears simultaneously along all the sample. The experimental transformation measurements suggest that the transformation passes from a local phenomenon to a global process.

In summary, for the first cycle of thick wires, a larger dissipation was observed when the front transformation extends under the wrapped thermocouple. After the training, or equivalently after a large number of working cycles, the dissipation is similar in all the samples (i.e., it can be defined "homogeneous").

5 | THICK DIAMETER WIRES: A THERMODYNAMIC INTERPRETATION

The previous section outlines that the training (or repeated working cycles) affects the way the transformation occurs. From a localized phenomenon, one moves to a distributed process. Therefore, the length of the sample should play a significant role.

Therefore, additional laboratory tests were carried out on the samples A1 and A2 of length 502 and 140 mm, respectively, after their training. This time, the strain step occurs in 2 s, and it is followed by 248 s of pause, for a total duration of the step of 250 s. The steps are only of the increasing type up to the 8% strain. Then the specimen is unloaded, and a sinusoidal cycle at 0.01 Hz follows.

The results collected for the short specimen are plotted in Figure 7, where emphasis is put on the Gaussian fit of the relation between step and temperature. Moving to the long specimen, Figure 8a and 8b shows the strain increases with the associated temperatures for each stepped cycle. As shown in Figure 8a, the associated temperature measurement against time was similar for the two K-thermocouples located at the top and bottom positions. But the temperature peaks clearly shown in of Figure 8b suggest that the long specimen was not completely homogeneous and shows two different behaviors.

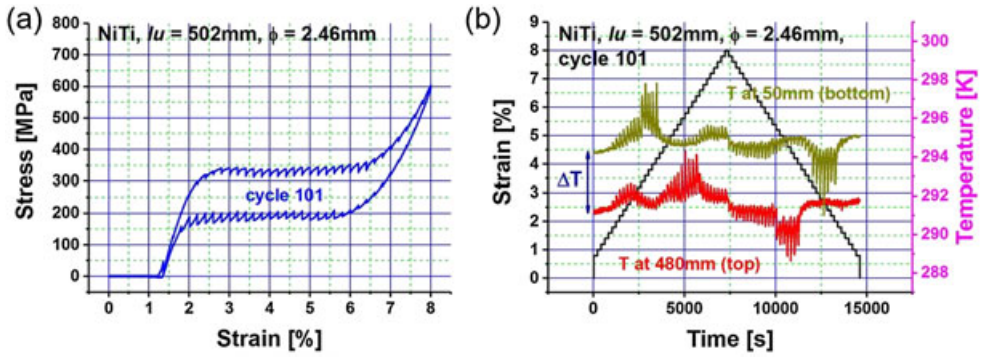

FIGURE 6 Strain steps effect after training: stress against strain (a), and temperatures against time (b)

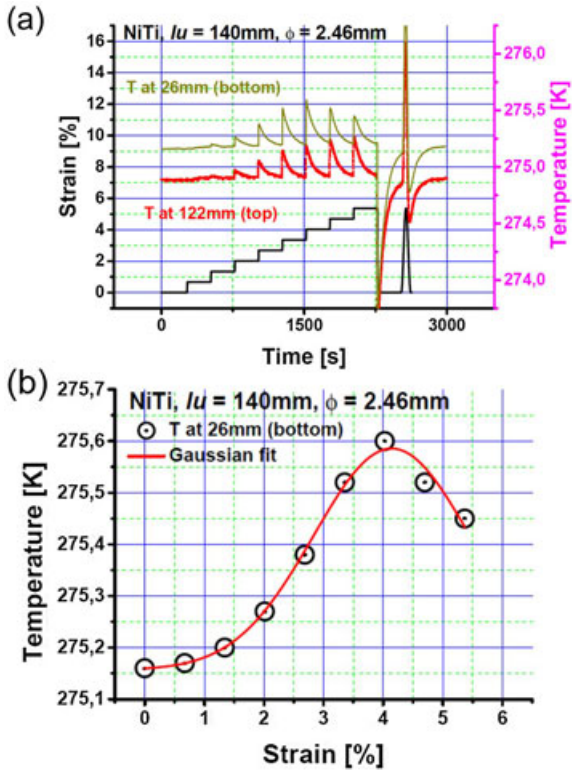

FIGURE 7 Strain steps and temperatures against time (a) and evolution of the temperature against strain (b)

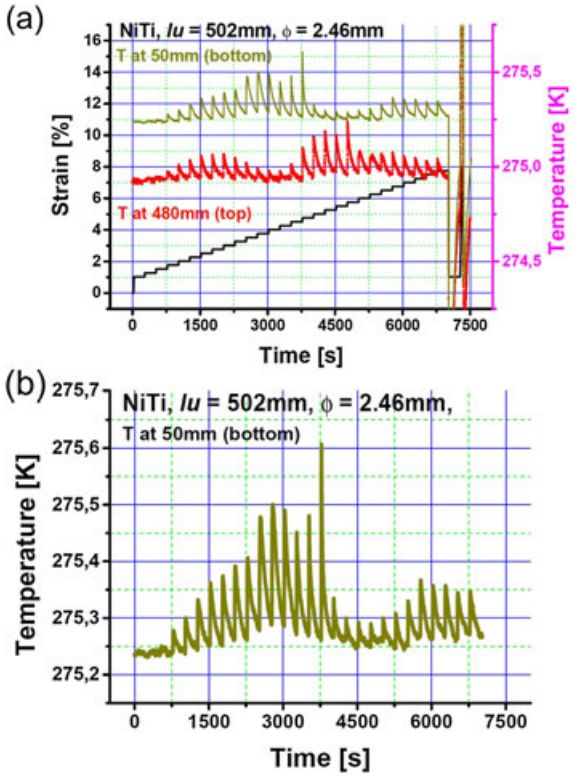

FIGURE 8 Strain steps and temperatures against time (a) and zoom on the temperature versus time (b)

In view of reading the results of these tests in terms of the thermodynamic equations of Section 2.2, one has to visualize the effect of $(dx/df)_{coex}$ in the S-shaped context. One detects a maximum. As this derivative is proportional to the heat capacity, the effect in the S-shaped context suggests the presence of an anomaly in the heat capacity. Actually, the measurements in Figure 7a (up to 2,000 or 2,100 s, just to simplify the reasoning) show a maximum in the temperature signal that can be tentatively associated to the heat capacity. Figure 8 goes in the direction of confirming this dependence, but a deeper study is in progress.

6 | CONCLUSIONS

This paper focuses attention on the critical discussion of macroscopic behaviors and temperature effects associated with the diameter of SMA wires.

The investigation covers several NiTi wires. The nonclassical S-shaped cycles shown by thick wires (i.e., 2.46 mm of diameter) state clear differences with the behavior of thinner samples (i.e., 0.5 mm).

In a classic phase transition, the transformation was realized at constant stress (as flat transformation in thinner wires). In this sense, the S-shaped cannot be considered as completely classical. The "particularity" of increasing transformation with increasing stress appears in the 80's in single interface transformation in CuZnA. A slope appears related with the dislocations concentration.

Detailed analyses suggest that these S-shaped measurements are not consistent with the classical consideration of the martensitic transformation (MT) as a first-order phase transition. In addition, the thermodynamics associated with the C-C equation, which requires flat transformations at constant force (or stress) and temperature, suggests a link in a coexistence zone between the strain–stress ratio and the specific heat. The results of the present experimental campaign also prove that the evolution from flat to S-shaped transformations relates a change from a local to a distributed dissipation. The temperature peaks associated with strain steps can be considered as indicative of an anomaly in the heat capacity for this type of specimens.

In view of SMA applications in dampers, the results outlined in the paper lead one to conclude that, during cold winter, the thinner wires are unappropriated for dissipating energy by hysteresis loops. In fact, such wires cannot retransform at very low temperatures. The positive effect of S-shaped loops, as shown by thick wires, can be exploited in cold winters areas, for instance down to −20 °C.

ACKNOWLEDGEMENT

Research Athenaeum Grants (FAR) from both the universities of Catania and Pavia are deeply acknowledged in supporting experiments and mobility. The first author also acknowledges the support by the PRIN2015 grant coordinated at a national level by Prof. M. Di Paola of the University of Palermo.

ORCID

M. Vece http://orcid.org/0000-0002-1697-0859

REFERENCES

[1] P. Ehrenfest, *Proceedings of the Royal Academy of Science at Amsterdam* **1933**, *36*, 153.

[2] L. D. Landau, *Phys. Z. Sowjetunion* **1937**, *11*, 26.

[3] F. C. Lovey, V. Torra, *Prog. Mater. Sci.* **1999**, *44*(3), 189.

[4] K. Otsuka, C. M. Wayman, *Shape Memory Materials*, Cambridge University Press, Cambridge, United Kingdom **1998**.

[5] C. M. Wayman, *Prog. Mater. Sci.* **1992**, *36*, 203.

[6] K. Otsuka, X. Ren, *Prog. Mater. Sci.* **2005**, *50*(5), 511.

[7] H. E. Mohammad, H. Mandi, T. Majid, S. B. Bhaduri, *Prog. Mater. Sci.* **2012**, *57*(5), 911.

[8] A. Ishida, M. Sato, A. Takei, S. Miyazaki, *Materials Transactions JIM* **1995**, *36*(11), 1349.

[9] J. I. Kim, H. Y. Kim, H. Hosoda, S. Miyazaki, H. Satoru, *Materials Transactions JIM* **2004**, *45*(7), 2443.

[10] J. I. Kim, H. Y. Kim, H. Hosoda, S. Miyazaki, *Materials Transactions JIM* **2005**, *46*(4), 852.

[11] H. Kanetaka, H. Hosoda, Y. Shimizu, T. Kudo, Y. Zhang, M. Kano, Y. Sano, S. Miyazaki, *Materials Transactions JIM.* **2010**, *51*(10), 1944.

[12] H. Janocha, *Adaptronics and smart structures*, Springer, Berlin, Germany **1999**.

[13] M. Kohl, *Microactuators*, Springer, Berlin, Germany **2004**.

[14] J. Van Humbeeck, *Mater. Sci. Eng., A* **1999**, *273*(275), 134.

[15] F. Casciati, C. Van derEijk, *Smart Structures and Systems* **2008**, *4*(2), 103.

[16] S. Casciati, K. Hamdaoui, *Smart Structures and Systems* **2008**, *4*(2), 153.

[17] F. Casciati, L. Faravelli, *Struct. Control Health Monit.* **2009**, *16*(7–8), 751.

[18] F. Casciati, L. Faravelli, R. Al Saleh, *Struct. Control Health Monit.* **2009**, *16*(6), 657.

[19] V. Torra, A. Isalgue, F. C. Lovey, M. Sade, *J. Therm. Anal. Calorim.* **2015**, *119*(3), 1475.

[20] V. Torra, C. Auguet, A. Isalgue, G. Carreras, P. Terriault, F. C. Lovey, *Engineering Structures* **2013**, *49*, 43.

[21] G. Carreras, F. Casciati, S. Casciati, A. Isalgue, A. Marzi, V. Torra, *Smart Structures and Systems* **2011**, *7*(1), 41.

[22] S. Casciati, A. Marzi, *Smart Structures and Systems* **2010**, *6*(1), 73.

[23] S. Casciati, L. Faravelli, M. Vece, *Struct. Control Health Monit.* **2017**, *24*(1), 1.

[24] S. Zhu, Y. Zhang, *Smart Mater. Struct.* **2007**, *16*(5), 1696.

[25] S. Zhu, Y. Zhang, *Earthquake and Structures* **2013**, *4*(6), 607.

[26] H. Prahlad, I. Chopra, *J. Intell. Mater. Syst. Struct.* **2003**, *14*, 429.

[27] A. Isalgue, V. Torra, A. Yawny, F. C. Lovey, *J. Therm. Anal. Calorim.* **2008**, *91*(3), 991.

[28] V. Torra, F. Martorell, Q. P. Sun, A. Ahadi, F. C. Lovey, M. Sade, *J. Therm. Anal. Calorim.* **2016**, *128*, 259, https://doi.org/10.1007/s10973-016-5886-8.

[29] V. Torra, G. Carreras, S. Casciati, P. Terriault, *Smart Structure Systems* **2014**, *13*(3), 353.

How to cite this article: Casciati S, Torra V, Vece M. Local effects induced by dynamic load self-heating in NiTi wires of shape memory alloys. *Struct Control Health Monit*. 2017;e2134. https://doi.org/10.1002/stc.2134